Approval Talk [HIG-23-005]

“Search for rare decays of the Higgs boson into a photon and a ρ^0, ϕ or K^{*0} meson”

R. Covarelli[1] M. Pellicciono[1] G. Umoret[1]
M. D’Alfonso[2] G. Gomez Ceballos[2] C. Paus[2] K. Yoon[2]

[1] Politecnico di Torino, Turin, Italy

[2] Massachusetts Institute of Technology, Cambridge, U.S.

March 19, 2024

About this analysis

FIX! add paper front page

HIG-23-005

Collaboration

- Collaboration of **MIT** and **Torino** groups, targeting different Higgs production categories.

Conveners

- **ARC**: Anadi Canepa (chair), Stefan Spanier, Jian Wang, Angelo Giacomo Zecchinelli
- **CCLE**: Christoph Maria Ernst Paus

Documentation

- Relevant links: CADI, TWiki, text
- Latest ANs (two individual + one combined):
  AN-22-004 (MIT, v9), AN-22-067 (Torino, v10), and AN-23-004 (combined, v7)

Introduction

Motivations

Higgs coupling with light quarks (u, d, s)

- Suppressed couplings and large QCD background hamper direct searches.
- Class of decays suggested $H \to M\gamma$, where M is a light-quark meson.
- *In this analysis*, $M = \phi, \rho^0, K^{*0}$ are considered.

Channel	Coupling	SM $\mathcal{BR}(H \to M\gamma)$
$H \to \phi\gamma$	s	$(1.68 \pm 0.08) \times 10^{-5}$ [1]
$H \to \rho^0\gamma$	u, d	$(2.31 \pm 0.11) \times 10^{-6}$ [1]
$H \to K^{*0}\gamma$	d&s (flavor-changing)	(Only available for $H \to d\bar{s} + \bar{d}s$) 1.19×10^{-11} [2]

Table 1: $H \to M\gamma$ channels considered in this analysis with their respective couplings and predicted branching ratios.

Motivations

$\mathbf{H \to M\gamma}$

- **Direct contribution**. The Higgs couples via Yukawa coupling to the quarks, one of which radiates a photon.
- **Indirect contribution**. The off-shell γ^* or Z^* produced in $H \to \gamma\gamma^*, \gamma Z^*$ *fragments* into a meson.

Direct and indirect contributions interfere destructively. Due to light quark masses, direct contribution is smaller than indirect. *Direct contribution is sensitive to deviation from SM.* Branching ratios are *typically* $\mathcal{O}(10^{-5}\text{–}10^{-6})$.

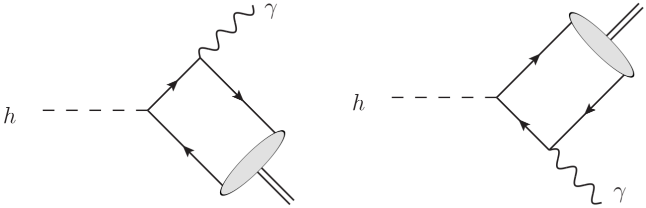

(a) Direct contributions via Yukawa coupling to the light quarks.

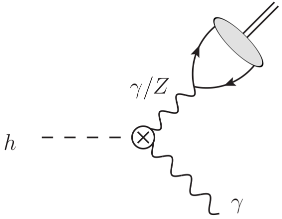

(b) Indirect contribution via a virtual photon or Z boson.

Figure 1: Leading order Feynman diagrams to the $H \to M\gamma$ processes. Image taken from Fig. 2 of [1].

Motivations

Flavor-conserving probes

- ϕ: s quark coupling (diagrams above)
- ρ^0: u and d quark coupling

Flavor-changing probe

- K^{*0}: flavor-changing s and d quarks via weak interaction (diagrams below)

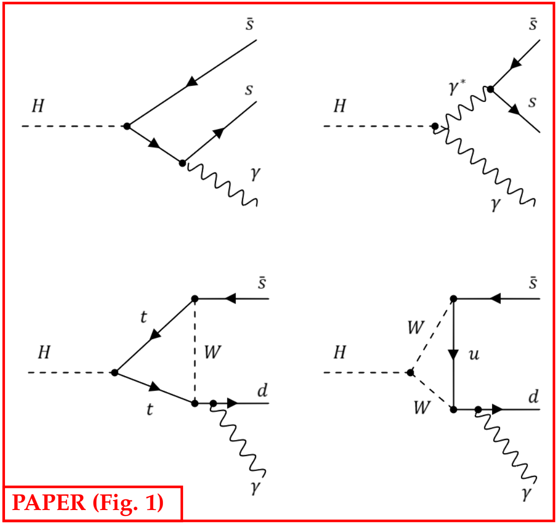

Figure 2: Feynman diagrams showing the different Higgs boson decay mechanisms into a photon and a light meson (top: ϕ meson; bottom: K^{*0} meson).

Analysis Strategy

- **Final states**
  1. High energy **photon**.
  2. High energy **di-track** from meson.

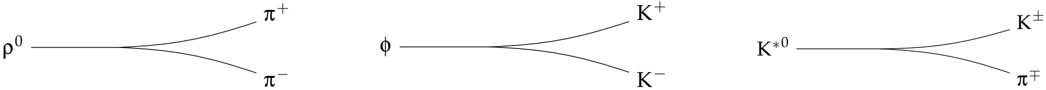

$\mathcal{BR}(\rho^0 \to \pi^+\pi^-) \sim= 100\%$ $\quad$ $\mathcal{BR}(\phi \to K^+K^-) \sim 49\%$ $\quad$ $\mathcal{BR}(K^{*0} \to K^\pm\pi^\mp) \sim 100\%$

Figure 3: Di-track systems for the different mesons considered in this analysis.

  3. Signal events extracted from **photon & di-track invariant mass spectrum**.

Analysis Strategy

- **Higgs Production Categories**

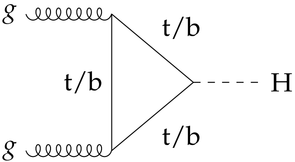

ggH

- No e/μ.

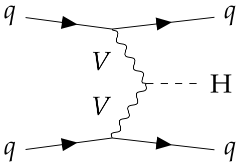

High-p_T^γ VBF

- $p_T^\gamma > 75$ GeV.
- No e/μ

Low-p_T^γ VBF

- $40 < p_T^\gamma < 75$ GeV.
- No e/μ

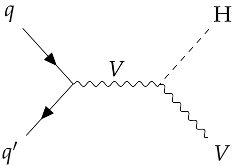

VH ($Z_{ll}H, W_{l\nu}H$)

- At least one e/μ.
- Also included is $t\bar{t}H$, accounting for $\sim 30\%$.

Triggers

Triggers

- **High Level Triggers (HLT)**
  Three types of triggers are employed.

Tau-like trigger

Photon + jets with τ-ID
$\rightarrow$ **ggH, low-p_T^{γ} VBF**

- Photon $p_T^{\gamma} > 35$ GeV + tau-like jet $p_T^{j} > 35$ GeV.
- Tau-leg similar to isolated di-track system.
- Active during 2018.

VBF-dedicated trigger

High-p_T^{γ} photon + VBF-like jets
$\rightarrow$ **high-p_T^{γ} VBF**

- Photon $p_T^{\gamma} > 35$ GeV + di-jet with large M_{jj} and $\Delta\eta_{jj}$.
- Active partly during 2016-17 and fully during 2018.

Leptonic trigger

Double or single lepton
$\rightarrow$ **VH**

- Single or double-muon (electron) lowest p_T thresholds vary depending on year.
- To complement selection, triggers requiring a lepton and a photon is also used.

- **High Level Triggers (HLT)**

	ggH	**High-p_T^{γ} VBF**	**Low-p_T^{γ} VBF**	**VH**
Triggers	tau-like	VBF-like	tau-like	single/di-muon single/di-electron muon+gamma
Luminosity (fb^{-1})	39.50 (2018)	28.2 (2016) 7.7 (2017) 60 (2018)	39.50 (2018)	138 (2016–2018)

Triggers

- **HLT Efficiencies and Scale Factors**
  Trigger efficiency **scale factor** defined as the ratio of data vs. MC efficiency.

$$\text{SF} = \frac{\epsilon_{\text{Data}}}{\epsilon_{\text{MC}}}$$

Triggers

- **HLT Efficiencies and Scale Factors**
  For the tau-like trigger, Data = Single Muon, MC = Drell-Yan. Photon-leg and tau-leg efficiencies measured separately, where
  FIX! do I need these equations?

$$\epsilon_{\gamma}^{\mathrm{HLT}} = \frac{\text{HLT\_Mu17\_Photon30} \wedge \text{offline selection} \wedge \text{HLT\_IsoMu24}}{\text{offline selection} \wedge \text{HLT\_IsoMu24}}$$

$$\epsilon_{\mathrm{TwoProngs}}^{\mathrm{HLT}} = \frac{\text{HLT\_IsoMu24\_TwoProngs35} \wedge \text{offline selection} \wedge \text{HLT\_IsoMu24}}{\text{offline selection} \wedge \text{HLT\_IsoMu24}}$$

Triggers

- **HLT Efficiencies and Scale Factors**
  Tau-like trigger efficiencies MC (blue) vs. Data (black).

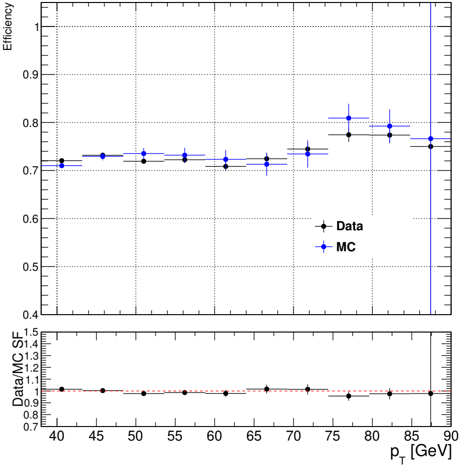

(a) Tau-like trigger photon-leg efficiencies for MC and data.

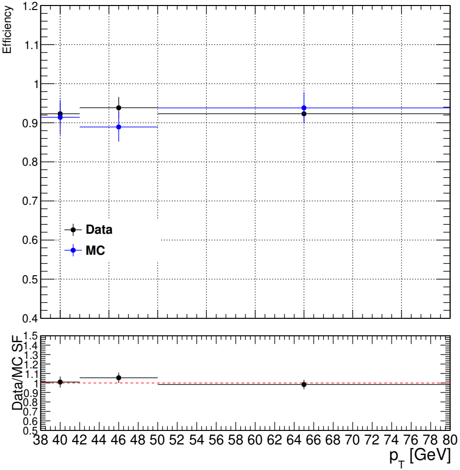

(b) Tau-like trigger tau-leg efficiencies for MC and data.

Figure 4: Photon-leg and tau-leg efficiencies of the tau-like trigger.

- **HLT Efficiencies and Scale Factors**
  VBF-dedicated trigger efficiencies MC (red) vs. Data (blue).

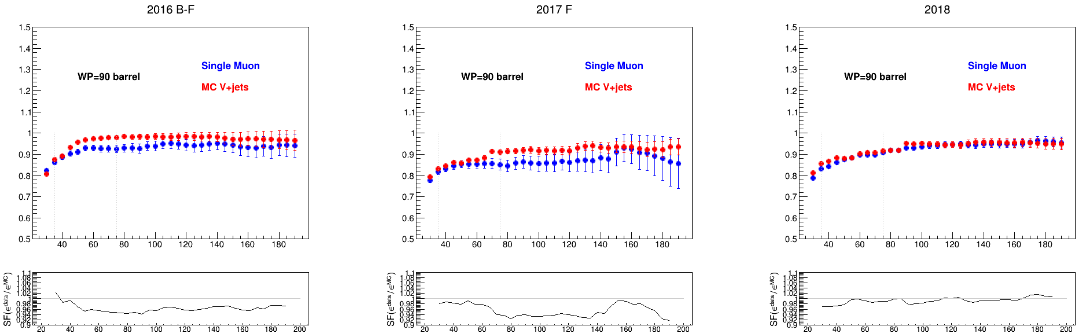

(a) VBF trigger photon-leg efficiencies for MC and data.

Figure 5: VBF-dedicated trigger photon-leg efficiencies for MC and data, shown for the $H \to \rho^0\gamma$ channel in 2016 (top-left), 2017 (top-right), and 2018 (bottom).

Simulated Samples

Simulated Samples

- **MC Generation**

  Gen-level: `POWHEG` (NLO) or `MADGRAPH5_aMC@NLC` (LO)
  PDFs: `NNPDF3.1` (NNLO)
  Hadronization: `PYTHIA 8.212`

- SM processes considered in background simulation are γ, W $\rightarrow$ lν, Drell-Yan Z $\rightarrow$ ll with jets, $t\bar{t}$, Wγ, and Zγ.

- Cross sections for Higgs production: FIX! double check

Process	σ (fb)
ggH	48580
VBF	3782
$W_{l\nu}H$	471
$Z_{ll}H$	77

Simulated Samples

- **Signal Simulation**

  Polarization reweighting of events.
  Higgs is a scalar, and angular momentum conservation constrains the mesons to have transverse spin alignment in the H $\rightarrow \mathrm{M}\gamma$ process. PYTHIA simulates unpolarized decay products. Therefore, signal events are reweighted by $(3/2)\sin^2\theta$, where θ is the angle between positive track in meson rest frame and meson flight direction in lab frame.

FIX! Which plot to include?

Event Selection

Event Selection

- **Photon selection**

	ggH	High-p_T^γ VBF	Low-p_T^γ VBF	VH
p_T^γ [GeV]	> 38	> 75	$38 < p_T^\gamma < 75$	> 40
$\lvert\eta^\gamma\rvert$	< 2.1	< 1.4	< 2.1	< 2.5
γ-ID signal eff.	80%	90%	80%	90%

Table 2: Photon selection criteria across different production categories.

- γ-ID signal eff. = MVA-based selection ID [3]
- p_T^γ cut based on trigger
- FIX! ggH & VH—**BUT PAPER IS NOT FIXED!** .
- ggH/VBF: conversion veto, VH: pixel veto.
- Highest-p_T^γ photon chosen as candidate.

Event Selection

- **Di-track system reconstruction**

Track selection

- Originate from PV.
- Pass "high purity" criteria.

Meson definition

- Pair of oppositely charged tracks.
- $p_T > 5$ GeV, $|\eta| < 2.5$.
- At least one track $p_T > 20$ GeV.

Invariant mass

- Di-track system invariant **mass windows and sidebands** (next slide).
- $K^{\pm}\pi^{\mp}$ system: if both combinations exist, then the one closest to $m_{\mathrm{K}^{*0}}$ is selected.
- Reject events where m_{KK} consistent with m_{π} and have higher p_T, vice versa.

Applies to all production categories.

Event Selection

- **Di-track system reconstruction**

Mass windows applied to invariant mass of di-track system.

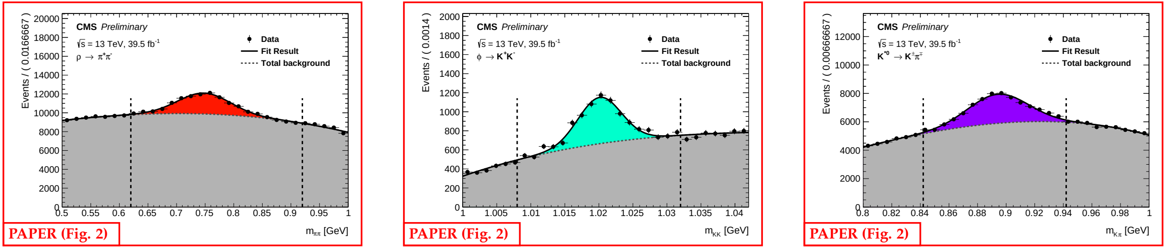

ρ^0 mass window: $0.62 < m_{\pi\pi} < 0.92$ GeV
Sidebands: $0.50 < m_{\pi\pi} < 0.62$ GeV
$0.92 < m_{\pi\pi} < 1.00$ GeV

ϕ mass window: $1.008 < m_{KK} < 1.032$ GeV
Sidebands: $1.000 < m_{KK} < 1.008$ GeV
$1.032 < m_{KK} < 1.050$ GeV

K^{*0} mass window: $0.84 < m_{K\pi} < 0.94$ GeV
Sidebands: $0.80 < m_{K\pi} < 0.84$ GeV
$0.94 < m_{K\pi} < 1.00$ GeV

Figure 6: Di-track mass distribution in selected events in data, for the ggH category of the analysis, $\rho^0\gamma$ (left), $\phi\gamma$ (middle) and $K^{*0}\gamma$ (right) channels. Vertical dashed lines represent the signal mass region borders.

FIX! Answer ARC MAR 05 question 2.

Event Selection

- **Di-track system selection**

Define the relative **charged isolation** of the leading meson candidate,

$$I^{\mathrm{trk}}(M) = \frac{p_T^{\mathrm{M}}}{p_T^{\mathrm{M}} + \sum_{\mathrm{trk}} |p_T^{\mathrm{trk}}|},$$

and the **neutral isolation** as

$$I^{\mathrm{neu}}(M) = \frac{p_T^{\mathrm{M}}}{p_T^{\mathrm{M}} + \sum_{\mathrm{neu}} |p_T^{\mathrm{neu}}|}.$$

$\sum_{trk/neu} |p_T^{trk/neu}|$: sum of charged/neutral track p_T within $\Delta R = 0.3$ of meson candidate.

	ggH	High-p_T^{γ} VBF	Low-p_T^{γ} VBF	VH
p_T^M [GeV]	> 38	> 40	> 40	> 40
I_M^{trk}	> 0.9	> 0.9	> 0.9	> 0.8
I_M^{neu}	> 0.8	-	-	-

Table 3: Di-track system criteria across different production categories.

Event Selection

- **Event tagging**

	ggH	**High-p_T^γ VBF**	**Low-p_T^γ VBF**	**VH**
Event tagging	Meson candidate within a jet with $p_T^j > 40$ GeV, tracks with $\Delta R < 0.07$	2 jets with $p_T^j > 40$ GeV, $m_{jj} > 400$ GeV, $\eta_{jj} > 3$	2 jets with $p_T^j > 30, 20$ GeV, $m_{jj} > 300$ GeV, $\eta_{jj} > 3$	1 selected and isolated e/μ or 2 selected e/μ compatible with m_Z

Table 4: Event tagging selection criteria across different production categories.

Summary of Event Selection

Common selections				
M selection	2 "high-purity" tracks, opposite sign $\lvert\eta^{\mathrm{trk}}\rvert < 2.5$, $p_T^{\mathrm{trk1}} > 20$ GeV, $p_T^{\mathrm{trk2}} > 5$ GeV, $\lvert\eta^{\mathrm{M}}\rvert < 2.1$ $0.62 < m_{\pi\pi} < 0.92$ GeV (ρ^0) / $1.008 < m_{\mathrm{KK}} < 1.032$ GeV (ϕ) / $0.84 < m_{\mathrm{K}\pi} < 0.94$ GeV (K^{*0})			
Category	ggH	VBF high-p_T^{γ}	VBF low-p_T^{γ}	VH
Trigger	Photon + jet with τ-ID	high-p_T photon + VBF-like jets	Photon + jet with τ-ID	Double or single lepton
p_T^{γ} [GeV]	> 38	> 75	> 40 and < 75	> 40
$\lvert\eta^{\gamma}\rvert$	< 2.5	< 1.4	< 2.1	< 2.5
γ-ID signal eff.	80%	90%	80/90%	90%
p_T^{M} [GeV]	> 38	> 30	> 38	> 38
$I^{\mathrm{trk}}(M)$	> 0.9	> 0.9	> 0.9	> 0.8
$I^{\mathrm{neu}}(M)$	> 0.8	-	-	-
Event tagging	Meson candidate within a jet with $p_T^{\mathrm{j}} > 40$ GeV, tracks with $\Delta R < 0.07$	2 jets with $p_T^{\mathrm{j}} > 40$ GeV $m_{\mathrm{jj}} > 400$ GeV $\lvert\Delta\eta_{\mathrm{jj}}\rvert > 3$	2 jets with $p_T^{\mathrm{j}} > 30/20$ GeV $m_{\mathrm{jj}} > 300$ GeV $\lvert\Delta\eta_{\mathrm{jj}}\rvert > 3$	1 selected and isolated e/μ or 2 selected e/μ compatible with Z mass
BDT categories				
cat0	BDT> 0.55	BDT> 0.7	BDT> 0.7	-
cat1	$-0.4 <$BDT< 0.55	$-0.6 <$BDT< 0.7	$-0.6 <$BDT< 0.7	-

PAPER (Table 1)

Figure 7: Summary of the event selections, including both common and category-specific selections.

MC/Data Background Comparison

content...

Multivariate Analysis Selection

Multivariate Analysis Selection

Multivariate Analysis (MVA) Overview

Motivation

Improvement of signal-to-background ratio in categories with backgrounds dominated by $\gamma +$ jet and multijet events. $\rightarrow$ **ggH**, **low-$\mathbf{p_T^\gamma}$ VBF**, and **high-$\mathbf{p_T^\gamma}$ VBF** categories.

Methodology

- BDT classifiers based on ROOT TMVA [4], optimized with the Gradient boosting method.
- Training and validation samples defined by **meson mass SR & sidebands**.
- Signal & Background events weighted by $1/(\sigma_M/M)$, where

$$\frac{\sigma_M}{M} = \sqrt{\left(\frac{\sigma_m}{m}\right)^2_{\text{meson}} + \left(\frac{\sigma_E}{E}\right)^2_\gamma}$$

FIX! match formula in paper

- BDT classification is further split into **two sub-categories** (“cat0” and “cat1”) based on optimized discriminator threshold values to improve upper limit results.
- FIX! write more stuff (e.g. cross-validation)

- **MVA Overview**

  Input variables:

	ggH	High-p_T^γ VBF	Low-p_T^γ VBF
Kinematics	p_T^γ p_T^M η_M	$p_T^{M\gamma}$ p_T^γ $p_T^M/m_{M\gamma}$	$p_T^{M\gamma}$ p_T^γ $p_T^M/m_{M\gamma}$
Meson Isolation	$I^{\mathrm{trk}}(\mathrm{trk}_1)$	$I^{\mathrm{trk}}(\mathrm{trk}_1)$	$I^{\mathrm{trk}}(\mathrm{trk}_1)$
Jet-related		M_{jj} $\Delta\phi_{\mathrm{jj}}$ z^*	M_{jj} $\Delta\phi_{\mathrm{jj}}$ z^*

Table 5: Input variables used for ggH and VBF categories.

z^* is the Zeppenfeld variable, defined as $z^* = |\eta_{M\gamma} - 0.5(\eta_{j1} + \eta_{j2})/|\Delta\eta_{jj}|$.

- **MVA: ggH category**
  - Training samples

    Signal: MC-generated
    Background: Data from meson mass sidebands.
  - 4 input variables

p_T^{γ}	photon p_T
p_T^{M}	meson p_T
η_{M}	meson η
$I^{\mathrm{trk}}(\mathrm{trk}_1)$	leading-track charged isolation

  - BDT sub-categories

    cat0: BDT-score > 0.55, optimized for max value of $S/\sqrt{B}$.
    cat1: $-0.4 <$ BDT-score < 0.55

Multivariate Analysis Selection

- **MVA: ggH category**
  - Training results:

FIX! possible to add cat0 and cat1 lines?

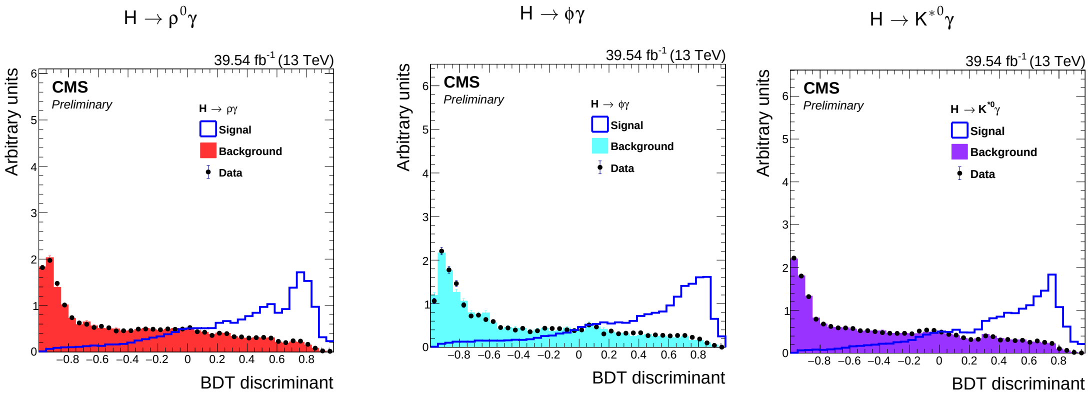

Figure 8: BDT-score shown for the three decay channels of ggH.

Multivariate Analysis Selection

- **MVA: High & Low-p_T^{γ} VBF categories**
  - Training samples

    Signal: MC-generated
    Background: γ+jets simulation and γ di-track events where the two tracks have the same charge.

  - 7 input variables
    Variable that is correlated with Higgs candidate mass is divided by the mass.

FIX! does not match with paper!

$p_T^{M\gamma}$	Higgs candidate p_T
p_T^{γ}	photon p_T
$p_T^{M}/m_{M\gamma}$	meson p_T divided by Higgs candidate mass
$I^{trk}(\mathrm{trk}_1)$	leading-track charged isolation
M_{jj}	di-jet invariant mass
$\Delta\phi_{jj}$	$\Delta\phi$ of the two jets
$z*$	Zeppenfeld variable

  - BDT sub-categories

    cat0: BDT-score > 0.7, optimized for max value of $S/\sqrt{B}$.
    cat1: $-0.6 <$ BDT-score < 0.7

Multivariate Analysis Selection

- **MVA: High-p_T^{γ} category**
  - Training results:

FIX! I NEED THE PLOT **FILES** (preferably pdf)

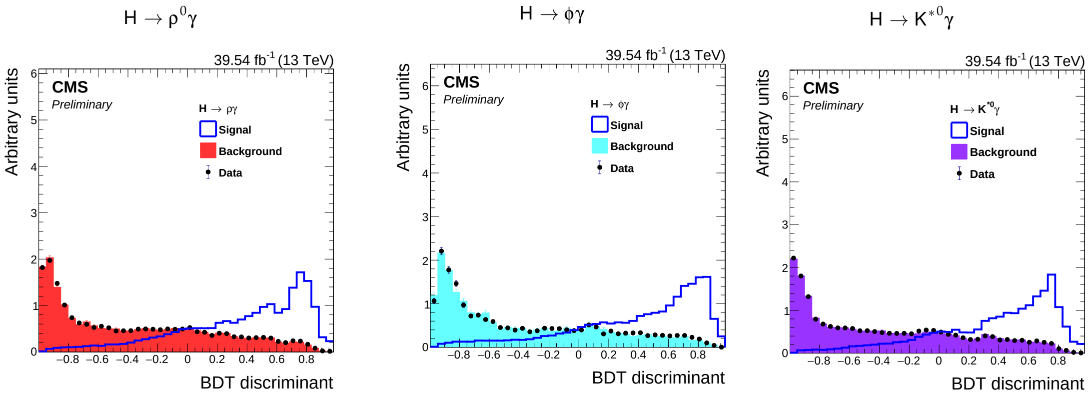

Figure 9: BDT-score shown for the three decay channels of High-p_T^{γ}.

Multivariate Analysis Selection

- **MVA: Low-p_T^{γ} category**
  - Training results:

FIX! I NEED THE PLOT **FILES** (preferably pdf)

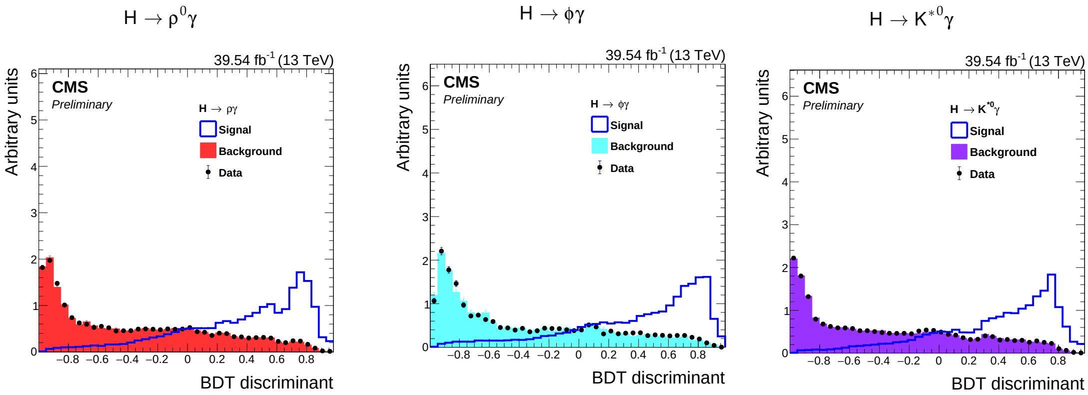

Figure 10: BDT-score shown for the three decay channels of Low-p_T^{γ}.

Signal Modeling & Systematic Uncertainties

Signal modeling

- Signal events extracted from the distribution of the **reconstructed Higgs boson mass**.
- Analytic function: **two-tailed Crystal Ball(TTCB)**.

$$\mathrm{TTCB}(t) = \begin{cases} e^{-t^2/2}, & \text{for } -\alpha_L < t < \alpha_R \\ (\frac{n_L}{|\alpha_L|})^{n_L} e^{-\alpha_L^2/2} (\frac{n_L}{|\alpha_L|} - |\alpha_L| - t)^{-n_L}, & \text{for } t \leq -\alpha_L \\ (\frac{n_R}{|\alpha_R|})^{n_R} e^{-\alpha_R^2/2} (\frac{n_R}{|\alpha_R|} - |\alpha_R| + t)^{-n_R}, & \text{for } t \geq \alpha_L \end{cases}$$

- Fitted via unbinned likelihood to simulated signal events.

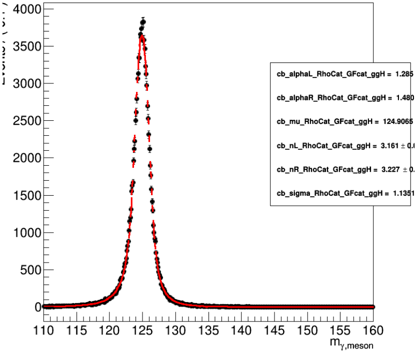

Figure 11: Example fitting of the TTCB function to the H $\to \rho^0\gamma$ selected signal samples in the ggH category.

Systematic Uncertainties

Integrated Luminosity	2.5% (2016), 2.3% (2017), and 2.5% (2018)
Total inelastic cross section	4.6%
Trigger efficiencies	VBF-dedicated trigger, 2.2-3.4% (photon-leg) and 5.3-5.6% (di-jet)
Photon ID efficiencies	Up to 1.5%, p_T and η dependent
Tracking efficiency	4.6-4.8% (2.3-2.6% FIX! ?? per track)
Muon/Electron ID	Less than 1.0% (muons) / 1.5% (electrons)
Meson Charged/Neutral Isolation Efficiencies	1.7-2.8 %, depending on search channel and isolation type
JEC & JES	Up to 3.5% in VBF, negligible in ggH
QCD renormalization and factorization	0.4% (VBF), 0.7% (WH), 3.8% (ZH), and 2.6% ($\mathrm{t\bar{t}H}$)
PDF & $\mathrm{ff_S}$	1.6-3.2%, depending on Higgs production
Parton shower modeling	FIX! what is the number?

Background modeling

- Analytic functions: **Chebychev** polynomials (main), **Bernstein** polynomials and **exponential** series (determination of shape uncertainties).
- Fitting region defined as $m_{M\gamma}$ sidebands.
    - ggH category: $110 < m_{M\gamma} < 120$ GeV & $130 < m_{M\gamma} < 160$ GeV.
    - VBF categories (high & low p_T^{γ}): $100 < m_{M\gamma} < 120$ GeV & $130 < m_{M\gamma} < 170$ GeV.
    - VH category: $100 < m_{M\gamma} < 120$ GeV & $130 < m_{M\gamma} < 150$ GeV.
- Degree of polynomial determined with **F-test**.
- **Bias test**.

Signal & Background Post-fit Distributions

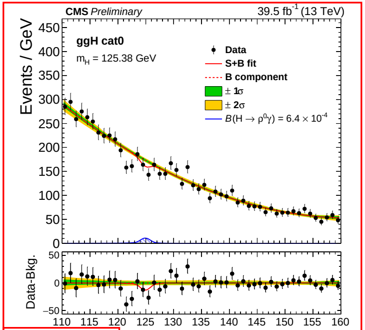

PAPER (Fig. 3)

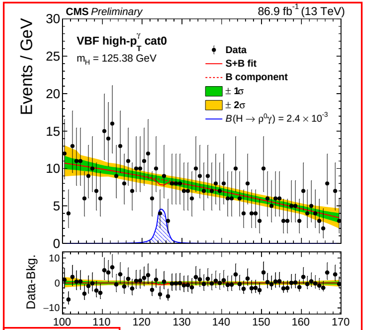

PAPER (Fig. 3)

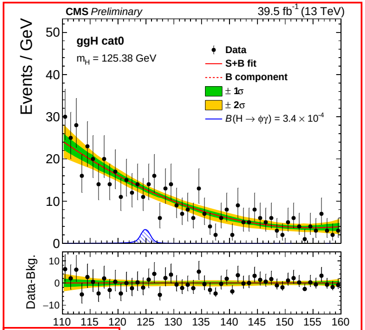

PAPER (Fig. 3)

Signal & Background Post-fit Distributions

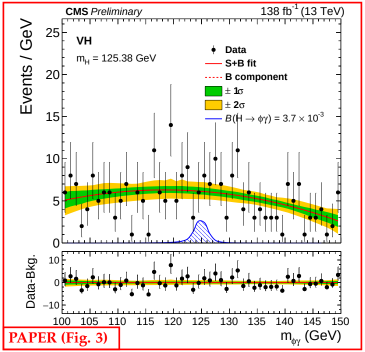

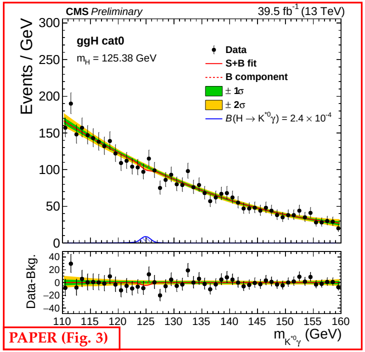

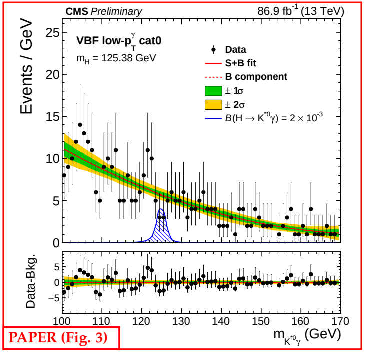

Results

Results

- **Upper limits** on $\mathcal{B}(H \to \rho^0\gamma)$, $\mathcal{B}(H \to \phi\gamma)$, and $\mathcal{B}(H \to K_0^*\gamma)$ set at 95% CL.
- CLs profile-likelihood ratio used as test-statistics, with the asymptotic approximation.
- Systematic uncertainties treated as nuisance parameters.

Results

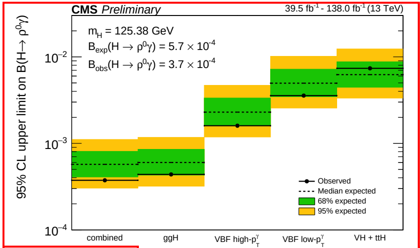

PAPER (Fig. 4)

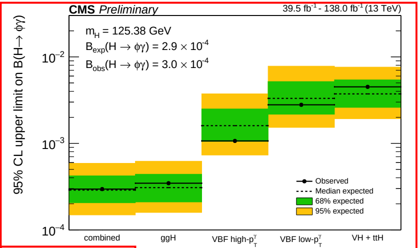

PAPER (Fig. 4)

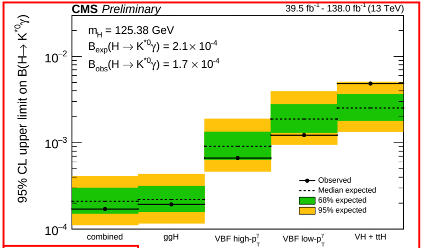

PAPER (Fig. 4)

Figure 14: Expected and observed upper limits on $\mathcal{B}(H \to \rho^0\gamma)$ (top left), $\mathcal{B}(H \to \phi\gamma)$ (top right), and $\mathcal{B}(H \to K_0^*\gamma)$ (bottom) split by analysis categories and combined. Green and yellow bands correspond to 1 and 2σ confidence intervals in the expected upper limits.

Results

	U.L. $\mathcal{B}(H \to \rho^0\gamma)$		U.L. $\mathcal{B}(H \to \phi\gamma)$		U.L. $\mathcal{B}(H \to K^{*0}\gamma)$	
category	Exp. (10^{-4})	Obs. (10^{-4})	Exp. (10^{-4})	Obs. (10^{-4})	Exp. (10^{-4})	Obs. (10^{-4})
VH	$62.3^{+25.6}_{-17.9}$	73.7	$37.3^{+16.9}_{-11.3}$	45.0	$25.3^{+11.4}_{-7.3}$	48.5
low-p_T^{γ} VBF	$49.6^{+22.5}_{-15.0}$	35.6	$33.1^{+18.7}_{-11.5}$	27.9	$18.8^{+8.90}_{-5.7}$	12.3
high-p_T^{γ} VBF	$22.9^{+10.5}_{-6.9}$	16.0	$16.0^{+9.0}_{-5.5}$	10.7	$9.13^{+4.25}_{-2.75}$	6.66
ggH	$6.01^{+2.53}_{-1.72}$	4.37	$3.08^{+1.33}_{-0.98}$	3.46	$2.20^{+0.94}_{-0.62}$	1.93
combined	$5.71^{+2.37}_{-1.63}$	3.74	$2.88^{+1.33}_{-0.83}$	2.97	$2.10^{+0.90}_{-0.58}$	1.71

PAPER (Table 2)

Figure 15: Exclusion limits at 95% CL on the branching fractions of the H boson decays. Observed and median expected limits with the upper and lower bounds in the expected 68% CL intervals are reported.

Results Comparison

Channel	Coupling	SM $\mathcal{BR}(H \to M\gamma)$	ATLAS Limits (10^{-4})	**Our Limits (10^{-4})**
$H \to \phi\gamma$	s	$(1.68 \pm 0.08) \times 10^{-5}$ [1]	Exp. $4.2^{+1.8}_{-1.2}$ Obs. 5.0 [5]	**Exp. $2.88^{+1.33}_{-0.83}$** **Obs. 2.97**
$H \to \rho^0\gamma$	u, d	$(2.31 \pm 0.11) \times 10^{-6}$ [1]	Exp. $10.0^{+4.9}_{-2.8}$ Obs. 10.4 [5]	**Exp. $5.71^{+2.37}_{-1.63}$** **Obs. 3.74**
$H \to K^{*0}\gamma$	$d\&s$ (flavor-changing)	(Only available for $H \to d\bar{s} + \bar{d}s$) 1.19×10^{-11} [2]	Exp. $3.7^{+1.5}_{-1.0}$ Obs. 2.2 [6]	**Exp. $2.10^{+0.90}_{-0.58}$** **Obs. 1.71**

Table 6: Comparison of branching ratios obtained from theory, ATLAS, and this analysis.

Bibliography

[1] M. König and M. Neubert, "*Exclusive radiative Higgs decays as probes of light-quark Yukawa couplings*", *Journal of High Energy Physics* **2015** (2015) .

[2] J.I. Aranda, G. González-Estrada, J. Montaño et al., "*Revisiting the rare $H \to q_i q_j$ decays in the standard model*", *Journal of Physics G: Nuclear and Particle Physics* **47** (2020) 125001.

[3] CMS collaboration, "*Electron and photon reconstruction and identification with the CMS experiment at the CERN LHC*", *Journal of Instrumentation* **16** (2021) P05014.

[4] A. Hoecker, P. Speckmayer, J. Stelzer et al., "*TMVA - Toolkit for Multivariate Data Analysis*", 2009.

[5] ATLAS collaboration, "*Erratum to: Search for exclusive Higgs and Z boson decays to $\phi\gamma$ and $\rho\gamma$ with the ATLAS detector*", *Journal of High Energy Physics* **2023** (2023) .

[6] ATLAS collaboration, "*Search for exclusive Higgs and Z boson decays to $\omega\gamma$ and Higgs boson decays to $K_0^*\gamma$ with the ATLAS detector*", *Physics Letters B* **847** (2023) 138292.